

Perivascular spaces—MRI marker of inflammatory activity in the brain?

Jens Wuerfel,^{1,*} Mareile Haertle,^{1,*} Helmar Waiczies,¹ Eva Tysiak,¹ Ingo Bechmann,² Klaus D. Wernecke,³ Frauke Zipp^{1,†} and Friedemann Paul^{1,†}

¹Cecilie Vogt Clinic for Neurology in the HKBB, Charité – Universitaetsmedizin Berlin, ²Dr Senckenbergische Anatomie, Institute of Clinical Neuroanatomy, Goethe University, Frankfurt and ³Sostana GmbH and Charité – Universitaetsmedizin Berlin, Germany

*These authors contributed equally to this work.

†These authors contributed equally to this work.

Correspondence to: Prof. Dr F. Zipp, Scientific Director of the Cecilie Vogt Clinic for Neurology in the HKBB, Charitéplatz 1, Charité – Universitaetsmedizin Berlin, 10117 Berlin, and Max-Delbrueck-Center for Molecular Medicine, Berlin, Germany
E-mail: frauke.zipp@charite.de

The Virchow–Robin spaces (VRS), perivascular compartments surrounding small blood vessels as they penetrate the brain parenchyma, are increasingly recognized for their role in leucocyte trafficking as well as for their potential to modulate immune responses. In the present study, we investigated VRS numbers and volumes in different brain regions in 45 multiple sclerosis patients and 30 healthy controls of similar age and gender distribution, applying three different MRI sequence modalities (T₂-weighted, T₁-weighted and FLAIR). VRS were detected in comparable numbers in both multiple sclerosis patients and healthy individuals, indicating that perivascular compartments present on MRI are not a unique feature of multiple sclerosis. However, multiple sclerosis patients had significantly larger VRS volumes than healthy controls ($P = 0.004$). This finding was not explained by a significantly lower brain parenchymal fraction (BPF), resulting from a higher degree of atrophy, in the patient cohort. In a multiple linear regression analysis, age had a significant influence on VRS volumes in the control group but not in multiple sclerosis patients ($P = 0.023$ and $P = 0.263$, respectively). A subsequent prospective longitudinal substudy with monthly follow-up MRI over a period of up to 12 months in 18 patients revealed a significant increase in VRS volumes and counts accompanying the occurrence of contrast-enhancing lesions (CEL). At time points when blood–brain barrier (BBB) breakdown was indicated by the appearance of CEL, total VRS volumes and counts were significantly higher compared with preceding time points without CEL ($P = 0.011$ and $P = 0.041$, respectively), whereas a decrease thereafter was not statistically significant. Thus, our data points to an association of VRS with CEL as a sign for inflammation rather than with factors such as age, observed in healthy controls, and therefore suggests a role of VRS in inflammatory processes of the brain.

Keywords: perivascular spaces; Virchow–Robin spaces; multiple sclerosis; MRI; neuroinflammation

Abbreviations: BBB = blood–brain barrier; BPF = brain parenchymal fraction; CEL = contrast-enhancing lesion; CNS = central nervous system; CSF = cerebrospinal fluid; EAE = experimental autoimmune encephalomyelitis; EDSS = expanded disability status scale; FLAIR = fluid-attenuated inversion recovery; IFN- β = interferon-beta; VRS = Virchow–Robin spaces

Received April 7, 2008. Revised July 4, 2008. Accepted July 4, 2008. Advance Access publication August 1, 2008

Introduction

The perivascular compartment surrounding small cerebral blood vessels (Virchow–Robin spaces, VRS) has been a focus of research for decades, although its role for lymphocyte trafficking into the brain was not appreciated until very recently (Greter *et al.*, 2005; van Horssen *et al.*, 2005; McMahon *et al.*, 2005; Cumurciuc *et al.*, 2006; Bechmann *et al.*, 2007). Owing to the complex topography of the

perivascular spaces, as illustrated in Fig. 1, two steps are considered necessary for cell invasion into the brain parenchyma: transmigration of the endothelium into the perivascular space and penetration through the glia limitans into the brain parenchyma. For the second step, it has been hypothesized that previously activated immune cells require restimulation (Tran *et al.*, 1998). In multiple sclerosis, a chronic inflammatory disease of the CNS, immune cell

Table 1 Demographic, clinical and MRI data of multiple sclerosis patients and healthy controls

	Multiple sclerosis patients	Controls
Male/Female	22/23	14/16
Age (years)	39.8 ± 8.2	37.8 ± 11.5
IMT (w/wo IFN-β)	32/13	NA
EDSS	2.3 ± 1.4	NA
Months since last relapse	16.7 ± 17.9	NA
Disease duration (years)	8.8 ± 6.2	NA
BH count	5.6 ± 8.4	NA
BH volume (mm ³)	556.9 ± 890.5	NA
T2 lesion count	479 ± 35.6*	4.5 ± 6.0*
T2 lesion volume (mm ³)	58279 ± 5445.2†	160.0 ± 283.0†
BPF	0.85 ± 0.04§	0.87 ± 0.02§
VRS count	34.4 ± 17.7	30.7 ± 22.4
VRS volume (mm ³)	280.8 ± 165.1§	210.8 ± 161.5§
Ratio VRS volume/BPF	331.3 ± 197.8#	242.0 ± 189.1#

Mean values and SD are presented.

* $P < 0.001$; † $P < 0.001$; § $P = 0.013$; # $P = 0.004$; # $P = 0.003$.

IMT = immunomodulatory treatment; BH = black hole;

BPF = brain parenchymal fraction; EDSS = expanded disability status scale; IFN-β = interferon-beta; NA = not applicable.

invasion leads to focal inflammatory and demyelinating lesions as well as axonal and neuronal damage (Frohman *et al.*, 2006; Zipp and Aktas, 2006). Although the exact pathogenesis of multiple sclerosis has not yet been elucidated, the current paradigm states that T cell activation is initiated in the peripheral lymphoid compartment. Once activated, T cells potentially enter the CNS via VRS, where they can be restimulated by antigen-presenting cells (Ransohoff *et al.*, 2003; Greter *et al.*, 2005; McMahon *et al.*, 2005; Becher *et al.*, 2006; Bechmann *et al.*, 2007). Perivascular cuffing (Gareau *et al.*, 2002) and VRS enlargement (Vos *et al.*, 2005) have been observed in multiple sclerosis and its animal model, experimental autoimmune encephalomyelitis (EAE) in post-mortem studies. Perivascular (Achiron and Faibel, 2002; Barkhof, 2004) or perivenular (Ge *et al.*, 2005) spaces detectable by MRI have also been described *in vivo* in physiological conditions such as the ageing brain as well as in multiple sclerosis. However, it is still a matter of debate as to whether VRS visible on MRI are a physiological feature or may be associated with multiple sclerosis. Therefore, this study aimed to address the following questions by means of a novel, 3D semi-automatic MRI approach: (i) does the presence of VRS on MRI distinguish multiple sclerosis patients from healthy controls?; (ii) do multiple sclerosis patients have more and/or larger VRS than healthy controls? and (iii) do VRS volumes change along with the appearance of contrast-enhancing lesions (CEL) indicating blood–brain barrier (BBB) leakage?

Material and methods

Participants

In this prospective study we enrolled 75 individuals, comprising 45 patients with relapsing–remitting multiple sclerosis, and a

Table 2 Demographic, clinical and MRI data of the 18 multiple sclerosis patients who participated in the longitudinal substudy

Male/Female	10/8
Age (years)	38.8 ± 6.5
EDSS	1.8 ± 1.1
Months since last relapse	7.0 ± 3.9
Disease duration (years)	8.3 ± 7.9
Number of monthly scans	7.5 ± 2.6
T2 lesion volume (mm ³) (CELneg.0I)	4213.4 ± 3369.6*
T2 lesion volume (mm ³) (CELpos.0I)	4868.5 ± 3484.3*
T2 lesion volume (mm ³) (CELpos.10)	4630.7 ± 3436.5 [‡]
T2 lesion volume (mm ³) (CELneg.10)	4377.1 ± 3405.3 [‡]
VRS volume (mm ³) (CELneg.0I)	151.2 ± 67.6 [§]
VRS volume (mm ³) (CELpos.0I)	177.3 ± 71.4 [§]
VRS volume (mm ³) (CELpos.10)	170.8 ± 90.2
VRS volume (mm ³) (CELneg.10)	149.8 ± 69.6
VRS count (CELneg.0I)	14.8 ± 6.1 [#]
VRS count (CELpos.0I)	18.2 ± 7.0 [#]
VRS count (CELpos.10)	17.3 ± 9.8
VRS count (CELneg.10)	14.9 ± 7.0
CEL volume (mm ³) (CELneg.0I)	8.8 ± 20.4 [§]
CEL volume (mm ³) (CELpos.0I)	278.4 ± 140.2 [§]
CEL volume (mm ³) (CELpos.10)	377.7 ± 522.6 [‡]
CEL volume (mm ³) (CELneg.10)	174 ± 23.8 [‡]
CEL count (CELneg.0I)	0.5 ± 0.9 [†]
CEL count (CELpos.0I)	2.4 ± 1.5 [†]
CEL count (CELpos.10)	1.7 ± 1.1 [‡]
CEL count (CELneg.10)	0.5 ± 0.5 [‡]

Mean values and SD are presented.

* $P = 0.001$; [‡] $P = 0.041$; [§] $P = 0.011$; # $P = 0.041$; [§] $P = 0.001$; [‡] $P < 0.001$;

[†] $P = 0.003$; [‡] $P = 0.003$.

CELneg.0I: scan without CEL at shift from 'CEL negative (0) → CEL positive (I)'.

CELpos.0I: scan with CEL at shift from 'CEL negative (0) → CEL positive (I)'.

CELpos.10: scan with CEL at shift from 'CEL positive (I) → CEL negative (0)'.

CELneg.10: scan without CEL at shift from 'CEL positive (I) → CEL negative (0)'.

control group of 30 healthy volunteers without history of neurological or psychiatric disease (Table 1). The two groups did not differ with respect to age or gender proportion. Patients were screened and enrolled in the outpatient clinic of the Cecilie Vogt Clinic for Neurology in the HKBB, Charité – Universitätsmedizin Berlin, and met the diagnostic criteria according to McDonald *et al.* (2001). The study was approved by the Charité Research Ethics Committee, and written informed consent was obtained from all participants according to the Declaration of Helsinki. There was no difference between multiple sclerosis patients and controls with respect to hypertension, migraine or smoking and none of the patients suffered from a relapse or received steroid treatment within 4 weeks prior to an imaging time point. A subgroup of 18 multiple sclerosis patients participated in a longitudinal follow-up study with monthly MRI over a period of up to 12 months (Table 2).

Magnetic resonance imaging

MRI measurements were performed on a 1.5 tesla scanner (Sonata, Siemens Medical Systems, Erlangen, Germany). T₂- and proton density-weighted images were obtained by a triple echo

spin–echo sequence (TR 5780 ms, TE₁ 13 ms, TE₂ 81 ms, TE₃ 121 ms, 3 mm slice thickness and 44 contiguous axial slices). Additionally, we applied a fluid-attenuated inversion recovery (FLAIR) sequence (TIRM, TR 10 000 ms, TE 108 ms, TI 2500 ms, 3 mm slice thickness and 44 contiguous axial slices) and a high resolution 3D T₁-weighted sequence (MPRAGE, TR 2110 ms, TE 4.38 ms, TI 1100 ms, flip angle 15°, resolution 1 mm³). Conventional spin–echo T₁-weighted (TR 1060 ms, TE 14 ms, 3 mm slice thickness and 44 contiguous axial slices) images were obtained before and 5 min after injection of 0.1 mmol/kg gadopentate dimeglumine (Gd-DTPA (Magnevist®), Bayer-Schering, Berlin, Germany). A series of axial, coronal and sagittal images was obtained to create a reference scan for subsequent accurate repositioning of patients at follow-up. Blinded MRI data analysis was performed following a semi-automatic procedure, which included an image coregistration (Jenkinson *et al.*, 2002) as well as an inhomogeneity correction routine embedded into the MedX3.4.3 software package (Medical Numerics, Germantown, USA). Time points with total CEL volumes greater than 100 mm³ were considered clearly CEL positive. Bulk white matter lesion load of T₂-weighted scans as well as number and volume of hypo- and hyperintense lesions on T₁-weighted scans were routinely measured using the MedX3.4.3 software package, as described previously (Wuerfel *et al.*, 2004). Brain parenchymal fraction (BPF) was calculated applying a fully automated software tool (Smith *et al.*, 2002), that yielded stable results in multiple sclerosis (Jasperse *et al.*, 2007).

Establishment of a novel VRS quantification paradigm

VRS are cerebrospinal fluid-filled (CSF) spaces ensheathing small blood vessels as they penetrate the brain parenchyma (Fig. 1A). They are enclosed by endothelial cells towards the blood vessel lumen and by astrocytic endfeet forming the glia limitans on the neuropil side (Fig. 1B and C). VRS were defined on MRI applying

three different sequence modalities after coregistration and inhomogeneity correction of the images, and could thus be differentiated from inflammatory lesions: (i) VRS were visualized as hyperintense regions on T₂-weighted sequences and as hypointense regions on T₁-weighted sequences (Fig. 2A and C). VRS within lesions were excluded to avoid partial volume contamination. Depending on the imaging plane, VRS formed punctuate or tubular structures of usually <3 mm in diameter. (ii) Anatomical tracing of blood vessels and VRS was achieved on high-resolution 3D isotropic T₁-weighted images (MPRAGE), and thus confirmed differentiation from multiple sclerosis lesions

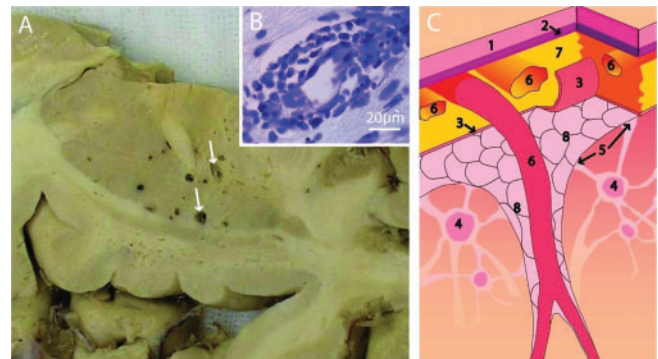


Fig. 1 The topography of VRS is presented in a post-mortem brain section. Arrows highlight VRS surrounding subcortical blood vessels (A). In a highly magnified toluidin blue-stained section (B) a small blood vessel is depicted, surrounded by cells that extravasated through the endothelium into the perivascular space. Very few cells crossed the glia limitans into the neuropil. The illustration (C) shows how the perivascular space is bordered by the outer vascular wall of cerebral vessels (6) and by astrocytic endfeet (5) forming the glia limitans (8) on the neuropil side. Dura mater (1), arachnoidea (2), pia mater (3), astrocytes (4) and the subarachnoid space (7) are marked.

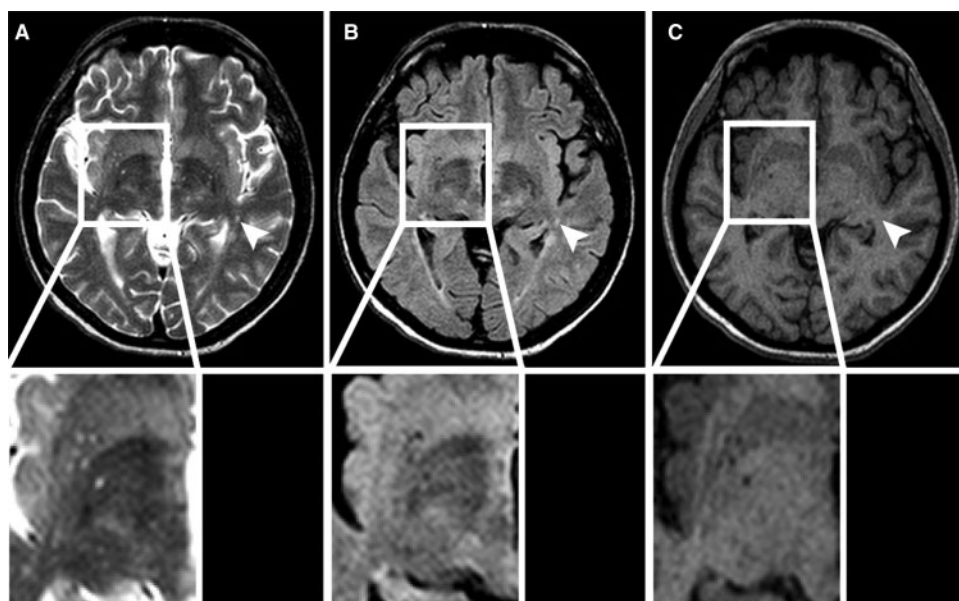


Fig. 2 VRS can be detected on different MRI sequences. VRS of the basal ganglia appear isointense to the CSF on axial T₂-weighted (A), FLAIR (B) and MPRAGE images (C), and are depicted below at a higher magnification. FLAIR imaging was used to distinguish multiple sclerosis lesions (arrow-head) from VRS; both present as hyperintensities on T₂-weighted images.

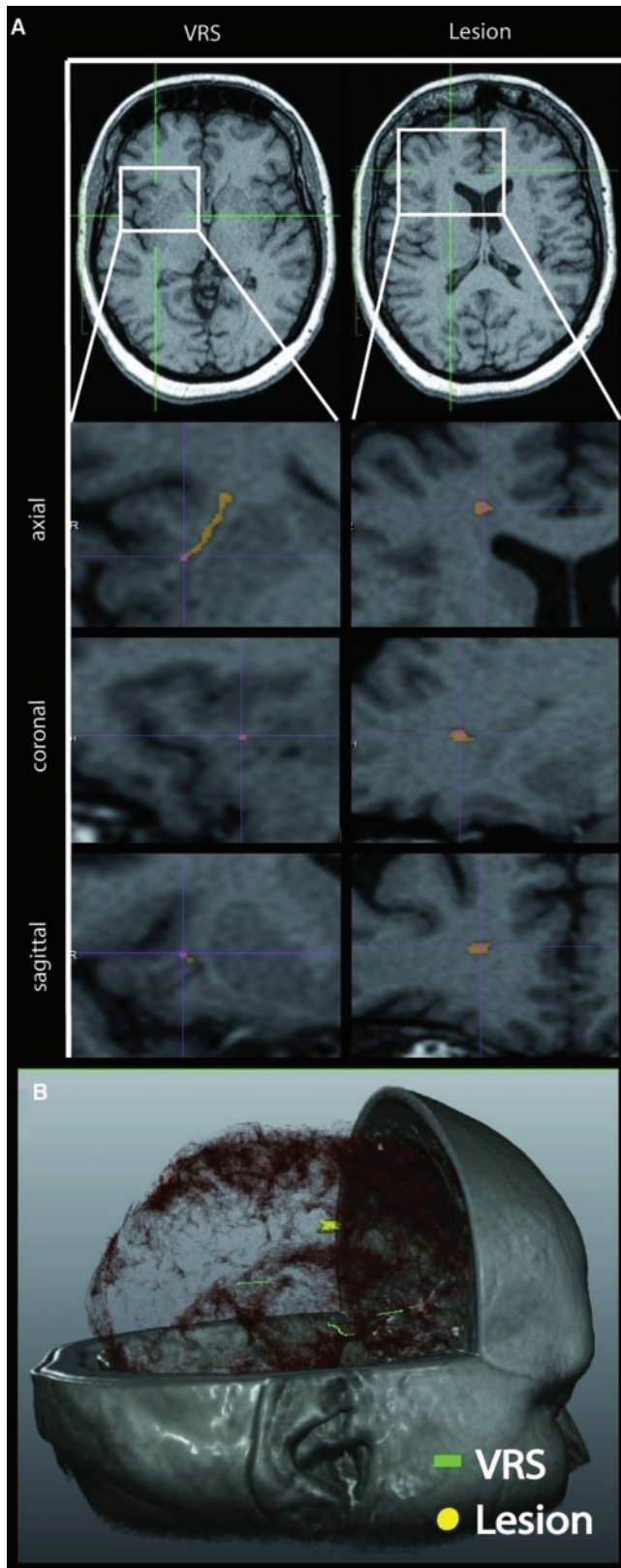


Fig. 3 The 3D volume images (MPRAGE) visualized the tubular structure of blood-vessel ensheathing VRS (**A**) and facilitated differentiation from small inflammatory lesions (**B**). Higher magnifications of the three main image planes are presented (**A**; axial, coronal and sagittal). The difference in the spatial

(Fig. 3A and B). VRS were typically located in conformity with the path of perforating brain vessels, which run perpendicular to the brain surface. (iii) On FLAIR, as in every other pulse sequence applied, VRS appeared isointense to CSF and could be easily differentiated from small inflammatory plaques (Fig. 2B). VRS were identified by two experienced raters (JW, MH) in consensus reading as clearly delineated hyperintense structures on corresponding T_2 -weighted scans, and both VRS numbers and volumes were quantified in a blinded fashion by applying a rater-independent threshold-based semi-automatic post-processing routine, embedded into the MedX3.4.3 software package following a procedure described elsewhere (Makale *et al.*, 2002). This software tool was further developed for multiple sclerosis lesion quantification, as recently reported (Wuerfel *et al.*, 2004; Paul *et al.*, 2008). For the quantification of very small structures such as VRS (average lesion diameter <3 mm), software parameters including connectivity and threshold values were adjusted and the results of the semi-automatic analysis were tested against manually determined VRS counts and volumes for validation purposes on four participants. As a result of practically identical measurements, comparison of semi-automatic versus manual quantification of VRS counts and volumes yielded an intra-class correlation coefficient of 1. Furthermore, VRS counts and VRS volumes were investigated in 10 randomly selected study participants by one experienced reader (MH) at two different time points to assess the intra-rater reliability of the semi-automatic quantification procedure. The intra-class correlation coefficient was 0.996 (95% CI 0.985–0.999) for VRS counts and 0.998 (95% CI 0.994–1.000) for VRS volumes.

Anatomy and histology

In order to show in principle the topography of VRS, a brain from the Frankfurt Brain Bank was cut in horizontal sections (Fig. 1A). Histological paraffin-sections derived from areas of inflammation were stained with toluidin blue. It has often been argued that VRS are artefacts of fixation, but we have previously demonstrated their functional connection to the subarachnoid space using tracer injections (Bechmann *et al.*, 2001a, b).

Statistical analysis

Results are expressed as arithmetic mean \pm SD. We applied the Mann–Whitney U-test to assess group differences between the two groups (multiple sclerosis patients versus healthy controls) in age, T2 lesion count, T2 lesion volume, BPF, VRS count, VRS volume and VRS volume/BPF ratio; and to assess group differences between patients with and without immunomodulatory therapy with IFN- β . Correlations between VRS counts and volumes on the one hand and age, EDSS, duration of disease and other MRI parameters on the other were calculated by Spearman's correlation coefficient. The Fisher exact test was used to test for differences regarding gender distribution between the multiple sclerosis and the control group. A multiple linear regression analysis was separately performed for both the multiple sclerosis and the

formation between small ball-shaped multiple sclerosis lesions and tubular VRS is not always obvious depending on the image plane (see sagittal and coronal versus axial slices in A), but can be easily appreciated in a 3D reconstruction (**B**). The 3D reconstruction was performed with MeVisLab SDK v1.6 (MeVisLab, Bremen, Germany).

healthy control groups to investigate the influence of age and BPF (independent variables) on VRS volumes and on VRS numbers (dependent variables). To assess the degree of agreement between semi-automatic and manual VRS number and volume quantification, the intra-class correlation coefficient was calculated using a one-way random model. Also intra-rater reliability of VRS number and volume quantification at two different time points was calculated by a one-way random model. In the longitudinal observation in 18 patients, Wilcoxon tests were applied to compare VRS volumes, VRS numbers, T2 lesion volumes, CEL volumes and CEL counts between two consecutive time points (months) that were defined by a shift from a CEL-negative scan to a CEL-positive scan ('CEL negative→CEL positive') or from a CEL-positive scan to a CEL-negative scan ('CEL positive→CEL negative'). One patient showed two 'CEL negative→CEL positive' shifts, 12 patients had one 'CEL negative→CEL positive' shift and 5 patients had no 'CEL negative→CEL positive' shift. Four patients showed two 'CEL positive→CEL negative' shifts, and 14 patients experienced only one 'CEL positive→CEL negative' shift. For reasons of clarity, we consistently included only the first 'CEL negative→CEL positive' shift and the first 'CEL positive→CEL negative' shift in our statistical analyses. A two-tailed P -value < 0.05 was considered statistically significant. All tests were performed as exploratory data analyses, such that no adjustments for multiple testing were made. The numerical calculations were performed with SPSS Version 13 (SPSS, Inc., Chicago, IL, USA) and SAS Version 9.1 (SAS Institute, Inc., Cary, NC, USA).

Results

VRS are detectable in healthy individuals and in multiple sclerosis patients

VRS were visualized predominantly in two brain regions: (i) the basal ganglia, encompassing lenticulostriate arteries and (ii) the cerebral high convexity along perforating blood vessels. VRS were detectable in the basal ganglia and the high convexity bilaterally in both multiple sclerosis patients and healthy controls, with the exception of two healthy volunteers who did not show subcortical VRS. Thus, the presence of VRS as such did not differentiate multiple sclerosis patients from healthy controls. Moreover, the number of VRS did not differ significantly between the two groups in any of the brain regions investigated (Table 1 and Fig. 4A). Figure 3A gives an example of VRS compared with multiple sclerosis plaques depending on the image plane and impression of their differential appearance in 3D space (Fig. 3B).

Multiple sclerosis patients present with larger VRS volumes compared with healthy controls

In contrast to the similar VRS counts, VRS volumes differed clearly between patients and controls. Multiple sclerosis patients presented with larger VRS bilaterally, resulting in significantly higher total VRS volumes ($P = 0.004$, Table 1 and Fig. 4B). None of the MRI parameters—such as number and volume of T2 lesions, or the number and volume of T1-hypointensities

('black holes')—correlated to VRS numbers and volumes. VRS numbers and volumes also did not correlate with disease duration, EDSS or the time since last relapse. Furthermore, VRS numbers and volumes did not differ between patients with or without immunomodulatory therapy. Interestingly, we found a significant positive correlation between VRS volumes and age only in the control group, i.e. VRS volumes increase with age ($r = 0.485$, $P = 0.007$). This significant correlation remained virtually unchanged when we repeated the calculation without one obvious outlier in the healthy control group ($r = 0.458$, $P = 0.013$). VRS volumes of multiple sclerosis patients do not, however, increase significantly with age ($r = 0.135$, $P = 0.377$). Concerning VRS counts, there was a significant positive correlation with age in the control group ($r = 0.370$, $P = 0.044$), while this did not hold true in the multiple sclerosis group ($r = 0.135$, $P = 0.377$).

Multiple sclerosis patients have smaller BPF but reveal no relation between these and VRS

Not surprisingly, and in line with previous reports (Miller et al., 2002), multiple sclerosis patients in our study had

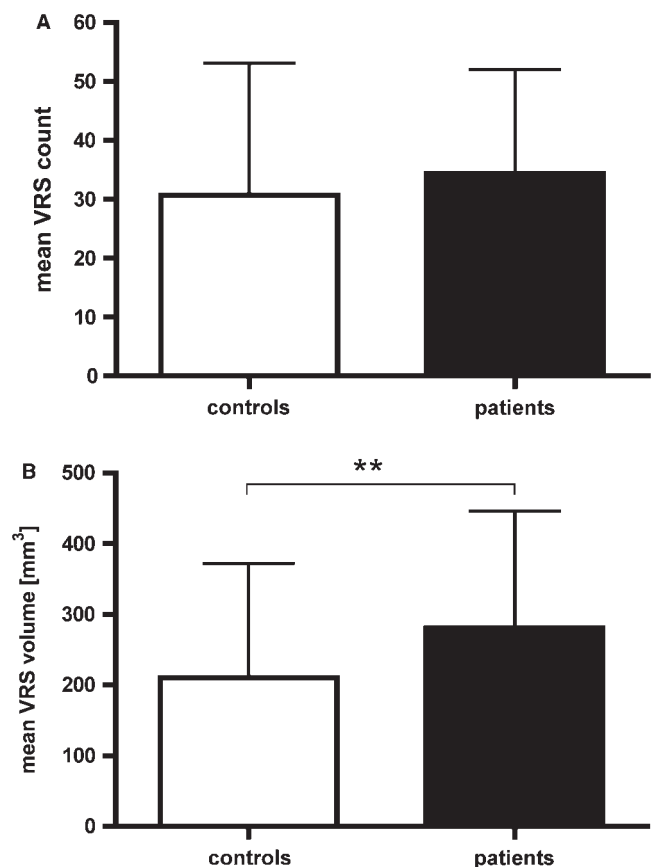


Fig. 4 VRS counts did not differentiate multiple sclerosis patients from healthy controls (A), but VRS volumes were significantly larger in multiple sclerosis patients (B; $**P = 0.004$). Mean values and SD are presented.

significantly lower BPF, indicating a higher degree of brain atrophy, as compared with healthy controls ($P=0.013$, Table 1 and Fig. 5). In the control group, there was a significant correlation between age and BPF, i.e. a decrease of BPF with increasing age ($r=-0.425$, $P=0.019$), while this did not hold true in the multiple sclerosis group ($r=-0.232$, $P=0.126$).

In the entire cohort as well as in both the multiple sclerosis and healthy controls group, there was no correlation between BPF on the one hand and VRS volumes and VRS counts on the other. We further calculated the VRS volume/BPF ratio, which was significantly higher in multiple sclerosis patients compared with controls ($P=0.003$, Table 1). The VRS volume/BPF ratio significantly increased with age only in the control group ($r=0.551$, $P=0.002$, Fig. 6) but not in the multiple sclerosis group ($r=0.178$, $P=0.242$, Fig. 6). In the multiple sclerosis group, multiple linear regression analyses did not reveal a significant influence of either age or BPF on either VRS volumes ($P=0.263$ and $P=0.513$, respectively) or on VRS counts ($P=0.376$ and $P=0.789$, respectively). In the control group, multiple linear regression analysis showed a significant influence of age, but not of BPF, on VRS volumes ($P=0.023$ and $P=0.455$, respectively) and VRS numbers ($P=0.020$ and $P=0.429$, respectively).

VRS volumes increase during acute inflammation

Following recent animal studies (Bechmann *et al.*, 2001a; Becher *et al.*, 2006), we investigated whether a shift from a CEL-negative to a CEL-positive scan at two consecutive time points indicating BBB breakdown was accompanied by changes in VRS volumes or VRS counts. In the 18 patients who participated in the longitudinal substudy, mean VRS volumes were significantly higher at time points of CEL occurrence compared with the preceding time points

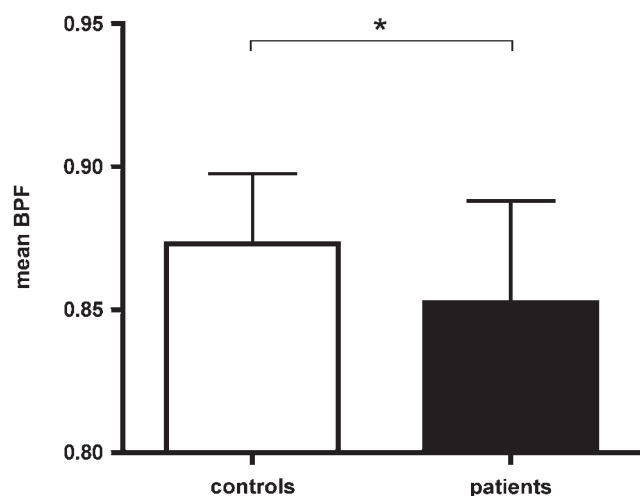


Fig. 5 BPF was significantly lower in multiple sclerosis patients (* $P=0.013$). Mean values and SD are presented.

without CEL (shift from 'CEL negative → CEL positive', $P=0.011$, Table 2 and Fig. 7A, left-hand image). The decrease of VRS volumes upon disappearance of CEL did not reveal statistical significance, however, at CEL-negative time points, VRS volumes were lower compared with the preceding CEL-positive time point (shift from 'CEL positive → CEL negative', $P=0.085$, Table 2 and Fig. 7A, right-hand image). Also mean VRS numbers were significantly higher at time points of CEL occurrence compared with the preceding time points without CEL (shift from 'CEL negative → CEL positive', $P=0.041$, Table 2 and Fig. 7B, left-hand image). The decrease of VRS numbers upon disappearance of CEL was not statistically significant, however, at CEL-negative time points, VRS numbers were lower compared with the preceding CEL-positive time point ($P=0.111$, Table 2 and Fig. 7B, right-hand image). T2 lesion load also increased when a shift from 'CEL negative → CEL positive' occurred ($P=0.001$, Table 2), and decreased when a shift from 'CEL positive → CEL negative' occurred ($P=0.041$, Table 2). In Fig. 8, the change in VRS size and number is shown between two time points prior to and during contrast enhancement (Fig. 8A and B, respectively). In none of our patients was meningeal contrast enhancement detected at any time point.

Discussion

In this study, we demonstrate increased size and disease-dependent changes of VRS volumes in multiple sclerosis patients versus healthy controls. In contrast to earlier investigations, we were able to reliably and reproducibly quantify not only subcortical VRS numbers, but also VRS volumes in different anatomical regions. By means of three different imaging modalities, VRS were clearly and

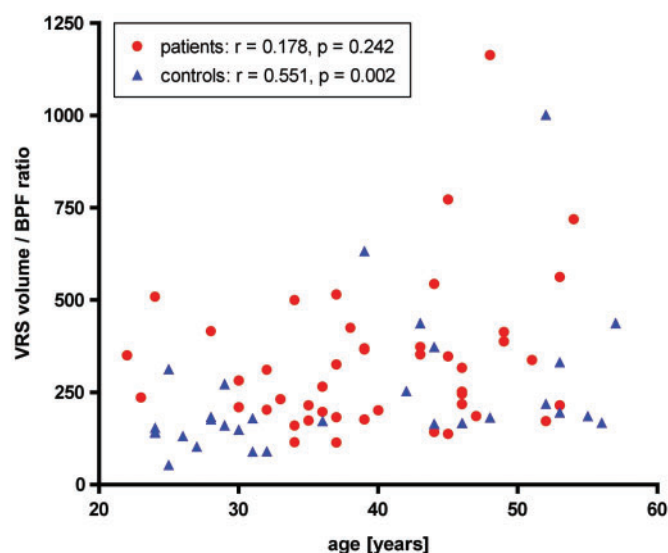


Fig. 6 In healthy individuals, the VRS volume/BPF ratio strongly correlates with age (blue triangles), while this is not the case in multiple sclerosis patients (red circles).

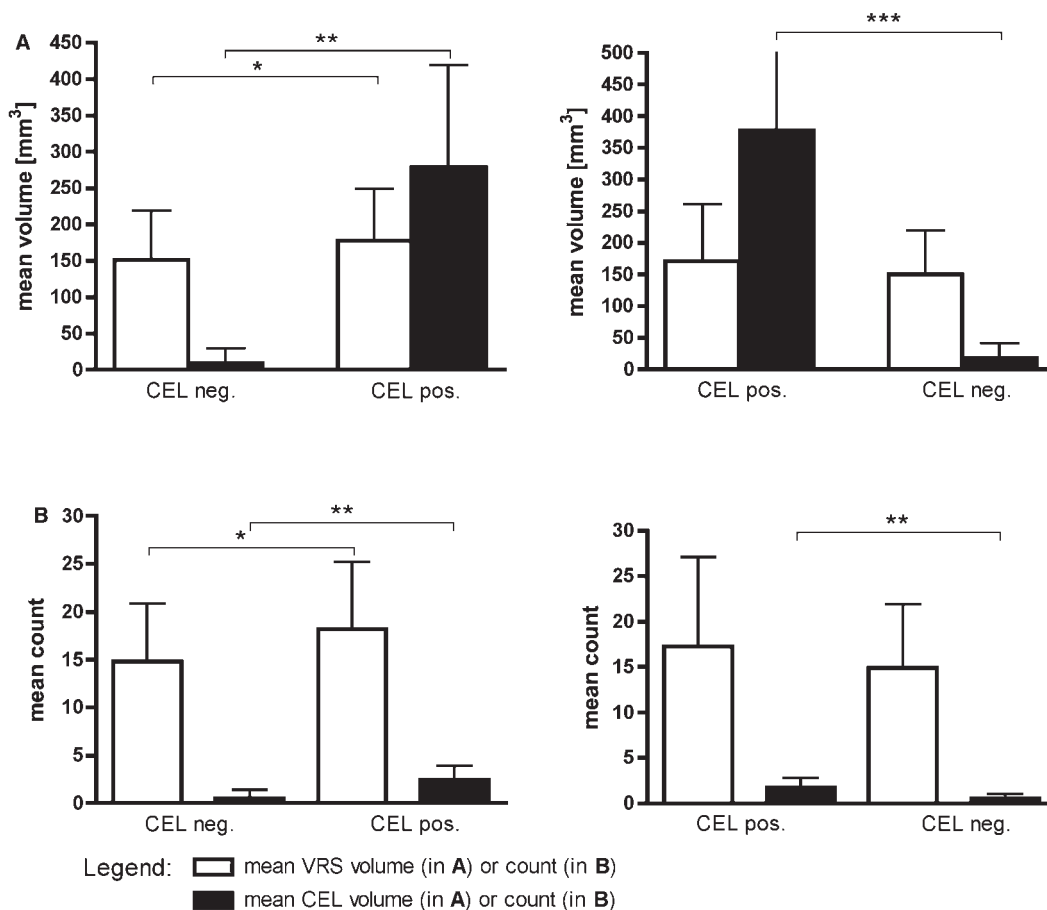


Fig. 7 A longitudinal substudy in 18 patients revealed significantly increased VRS volumes at time points of BBB breakdown with contrast enhancement compared with preceding time points without contrast enhancement (**A**, left-hand image; CEL negative→CEL positive, $*P=0.011$). In parallel with a shift from a CEL-positive time point to a CEL negative time point, VRS volumes did not decrease significantly (**A**, right-hand image; CEL positive→CEL negative, $P=0.085$). VRS counts also significantly increased at time points of BBB breakdown with contrast enhancement compared with preceding time points without contrast enhancement (**B**, left-hand image; CEL negative→CEL positive, $*P=0.041$). In parallel with a shift from a CEL-positive to a CEL-negative time point, VRS numbers did not decrease significantly (**B**, right-hand image; CEL positive→CEL negative, $P=0.111$). Mean values and SD are presented.

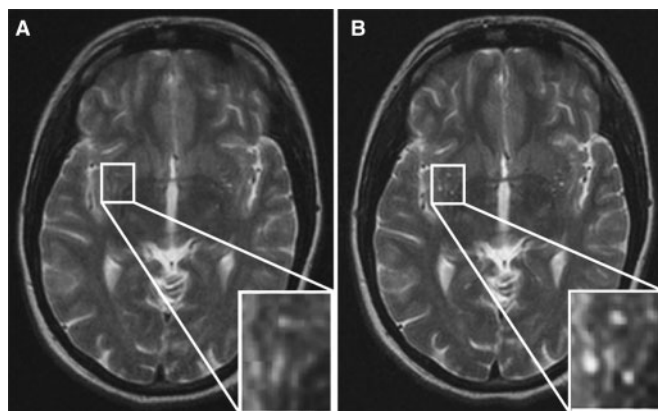


Fig. 8 T₂-weighted images of the same slice position from one study participant at two different time points are shown and magnified (inserts) (**A**: 4 weeks prior to BBB breakdown; **B**: in the presence of CEL) to show the alteration in VRS size and number. A semi-automatic threshold-based software was used to quantify the differences.

systematically distinguished from inflammatory lesions. We showed that (i) in contradiction to previous proposals, the presence of VRS as such is not specific or pathognomonic for multiple sclerosis, but is a physiological phenomenon also detectable in healthy individuals; (ii) VRS are significantly larger in multiple sclerosis patients compared with healthy controls and (iii) VRS volumes and numbers increase when CEL indicating BBB disruption appear on MRI. Despite growing interest in the presumed role of VRS in immune surveillance (Bechmann *et al.*, 2001b; Man *et al.*, 2007; McCandless and Klein, 2007), *in vivo* imaging of VRS by MRI has been widely neglected until very recently. One study examined VRS in multiple sclerosis patients (Achiron and Faibel, 2002) and suggested these perivascular spaces as a novel neuroradiologic *in vivo* marker for multiple sclerosis, as a consequence of the finding that a significantly higher proportion of multiple sclerosis patients presented with subcortical VRS compared with controls. In that study, however, and in contrast to

our methods, only two subcortical slices were applied, thus omitting the basal ganglia, and VRS volumes were not compared between groups.

Noteworthy is our finding of significantly higher VRS volumes in multiple sclerosis patients compared with controls despite equal VRS numbers in both groups. One could presume that the higher VRS volumes detected in the multiple sclerosis group might be a result of internal atrophy. In accordance with the literature (Miller *et al.*, 2002), multiple sclerosis patients in our study presented with a higher degree of brain atrophy compared with healthy individuals. However, a significant correlation between VRS volumes, BPF and the VRS volume/BPF ratio on the one hand and age on the other held true only in the control group and not in patients. Moreover, the multiple linear regression analysis revealed a significant influence of age on VRS volumes only in the control group, but not in multiple sclerosis patients. This strongly argues against a mere effect of age or age-related brain volume reduction as the major reason for an increase of VRS volumes in multiple sclerosis patients (Heier *et al.*, 1989; MacLulich *et al.*, 2004). In addition, enlarged VRS in multiple sclerosis patients are not explained by disease-related brain atrophy either, as our multiple linear regression analysis did not show a significant influence of brain atrophy on VRS volumes in our patient group. We hypothesized that inflammatory activity leading to infiltration of cells and edema may lead to an enlargement of VRS, resulting in larger VRS volumes and thus also in an increased number of VRS detectable by MRI. Indeed, in our longitudinal observation we found that VRS volumes and numbers significantly increased upon development of BBB disruption, namely contrast enhancement. As the calculated intra-class coefficients showed an excellent intra-rater reliability in our blinded VRS quantification procedure, technical and methodological artefacts are unlikely to influence these changes in VRS volumes and numbers. The fact that there is no significant decrease in VRS volumes and numbers parallel to the disappearance of contrast enhancement suggests that reduction of VRS volumes and counts may lag behind the cessation of contrast enhancement, as we have recently shown for changes in cerebral perfusion at the site of an active lesion (Wuerfel *et al.*, 2004). In sum, despite its exploratory character and thus without making adjustments for multiple testing, our study may indicate that VRS are sites where inflammatory activity is triggered in the CNS.

This assumption is supported by recent experimental data and animal studies. An interaction between immune cells and those of the nervous system is part of a general host defence, and plays an essential role in protecting the CNS from chronic infections and pathogen-induced damage. Therefore, the immune system and the nervous system can no longer be viewed as two compartments sealed off from each other by a tight barrier impeding communication. The CNS is continuously patrolled by

lymphocytes, which—under ‘healthy’ conditions—do not lead to inflammation or alterations of BBB integrity (Brabb *et al.*, 2000; Hickey, 2001; Ransohoff *et al.*, 2003; Man *et al.*, 2007; Smorodchenko *et al.*, 2007). However, when lymphocytes activated in the context of a local infectious or autoimmune process re-encounter their specific antigens (Hickey and Kimura, 1988), most probably presented within the CNS by perivascular antigen-presenting cells (Hickey and Kimura, 1988; Greter *et al.*, 2005; McMahon *et al.*, 2005; Becher *et al.*, 2006), these lymphocytes may initiate an inflammatory response. This response may then promote BBB disruption and the invasion of leucocytes attracted into CNS parenchyma (Hickey, 1991). These are two key manifestations of early disease stages in multiple sclerosis and its animal model EAE (Kermode *et al.*, 1990), although the primary site of BBB leakage may topographically differ between multiple sclerosis and EAE, as meningeal contrast enhancement is rarely detected in multiple sclerosis, but not uncommon in animal models (Traboulsee and Li, 2006). The perivascular space is potentially one of the most important entry routes of soluble proteins as well as of leucocytes into the CNS (Ransohoff *et al.*, 2003). Within the current concept, VRS directly communicate with the subarachnoid space, and are thus partly filled with CSF. Their outer boundary is formed by a single layer of invaginated pia, and the inner by the tunica adventitia. Histopathologic studies showed that, in addition to dendritic cells and perivascular microglia, T cells are physiologically located within these spaces (Bechmann *et al.*, 2001a; Greter *et al.*, 2005; McMahon *et al.*, 2005), predestining VRS for a key role in immune surveillance (Engelhardt and Ransohoff, 2005). During the generation and maintenance of inflammatory processes (Greter *et al.*, 2005; McMahon *et al.*, 2005; Becher *et al.*, 2006; Bechmann *et al.*, 2007), these spaces may dilate and become more easily visible owing to cell and fluid accumulation. A recent post-mortem study in multiple sclerosis patients lent further weight to this evidence: Vos *et al.* (2005) demonstrated enlarged VRS containing infiltrated leucocytes associated with diffusely abnormal white matter and focal abnormalities on post-mortem MRI. Furthermore, applying MR microscopy, Gareau *et al.* (2002) described perivascular cell accumulations during acute inflammation in post-mortem EAE slices. To our knowledge, this is the first longitudinal study to investigate short-term fluctuations in VRS volumes and, more importantly, to correlate these to occurrence and disappearance of CEL. Our findings suggest that enlarged VRS—although not a unique feature of multiple sclerosis—may be involved in neuroinflammatory activity.

Acknowledgements

This work was supported by grants of the German Federal Ministry of Education and Research (BMBF) and of the Institute for Multiple Sclerosis Research Göttingen

(IFMS) to F.Z. We wish to thank Alistair Noon for carefully editing the manuscript as an English native speaker.

References

- Achiron A, Faibel M. Sandlike appearance of Virchow-Robin spaces in early multiple sclerosis: a novel neuroradiologic marker. *Am J Neuroradiol* 2002; 23: 376–80.
- Barkhof F. Enlarged Virchow-Robin spaces: do they matter? *J Neurol Neurosurg Psychiatry* 2004; 75: 1516–7.
- Becher B, Bechmann I, Greter M. Antigen presentation in autoimmunity and CNS inflammation: how T lymphocytes recognize the brain. *J Mol Med* 2006; 84: 532–43.
- Bechmann I, Galea I, Perry VH. What is the blood-brain barrier (not)? *Trends Immunol* 2007; 28: 5–11.
- Bechmann I, Kwidzinski E, Kovac AD, Simburger E, Horvath T, Gimsa U, et al. Turnover of rat brain perivascular cells. *Exp Neurol* 2001; 168: 242–9.
- Bechmann I, Priller J, Kovac A, Bontert M, Wehner T, Klett FF, et al. Immune surveillance of mouse brain perivascular spaces by blood-borne macrophages. *Eur J Neurosci* 2001; 14: 1651–8.
- Brabb T, von Dassow P, Ordonez N, Schnabel B, Duke B, Goverman J. In situ tolerance within the central nervous system as a mechanism for preventing autoimmunity. *J Exp Med* 2000; 192: 871–80.
- Cumurciuc R, Guichard JP, Reizine D, Gray F, Bousser MG, Chabriat H. Dilation of Virchow-Robin spaces in CADASIL. *Eur J Neurol* 2006; 13: 187–90.
- Engelhardt B, Ransohoff RM. The ins and outs of T-lymphocyte trafficking to the CNS: anatomical sites and molecular mechanisms. *Trends Immunol* 2005; 26: 485–95.
- Frohman EM, Racke MK, Raine CS. Multiple sclerosis—the plaque and its pathogenesis. *N Engl J Med* 2006; 354: 942–55.
- Gareau PJ, Wymore AC, Cofer GP, Johnson GA. Imaging inflammation: direct visualization of perivascular cuffing in EAE by magnetic resonance microscopy. *J Magn Reson Imaging* 2002; 16: 28–36.
- Ge Y, Law M, Herbert J, Grossman RI. Prominent perivenular spaces in multiple sclerosis as a sign of perivascular inflammation in primary demyelination. *Am J Neuroradiol* 2005; 26: 2316–9.
- Greter M, Heppner FL, Lemos MP, Odermatt BM, Goebels N, Laufer T, et al. Dendritic cells permit immune invasion of the CNS in an animal model of multiple sclerosis. *Nat Med* 2005; 11: 328–34.
- Heier LA, Bauer CJ, Schwartz L, Zimmerman RD, Morgello S, Deck MD. Large Virchow-Robin spaces: MR-clinical correlation. *Am J Neuroradiol* 1989; 10: 929–36.
- Hickey WF. Migration of hematogenous cells through the blood-brain barrier and the initiation of CNS inflammation. *Brain Pathol* 1991; 1: 97–105.
- Hickey WF. Basic principles of immunological surveillance of the normal central nervous system. *Glia* 2001; 36: 118–24.
- Hickey WF, Kimura H. Perivascular microglial cells of the CNS are bone marrow-derived and present antigen in vivo. *Science* 1988; 239: 290–2.
- Jasperse B, Valsasina P, Neacsu V, Knol DL, De Stefano N, Enzinger C, et al. Intercenter agreement of brain atrophy measurement in multiple sclerosis patients using manually-edited SIENA and SIENAX. *J Magn Reson Imaging* 2007; 26: 881–5.
- Jenkinson M, Bannister P, Brady M, Smith S. Improved optimization for the robust and accurate linear registration and motion correction of brain images. *Neuroimage* 2002; 17: 825–41.
- Kermode AG, Thompson AJ, Tofts P, MacManus DG, Kendall BE, Kingsley DP, et al. Breakdown of the blood-brain barrier precedes symptoms and other MRI signs of new lesions in multiple sclerosis. Pathogenetic and clinical implications. *Brain* 1990; 113 (Pt 5): 1477–89.
- MacLulich AM, Wardlaw JM, Ferguson KJ, Starr JM, Seckl JR, Deary IJ. Enlarged perivascular spaces are associated with cognitive function in healthy elderly men. *J Neurol Neurosurg Psychiatry* 2004; 75: 1519–23.
- Makale M, Solomon J, Patronas NJ, Danek A, Butman JA, Grafman J. Quantification of brain lesions using interactive automated software. *Behav Res Meth Instrum Comput* 2002; 34: 6–18.
- Man S, Ubogu EE, Ransohoff RM. Inflammatory cell migration into the central nervous system: a few new twists on an old tale. *Brain Pathol* 2007; 17: 243–50.
- McCandless EE, Klein RS. Molecular targets for disrupting leukocyte trafficking during multiple sclerosis. *Expert Rev Mol Med* 2007; 9: 1–19.
- McDonald WI, Compston A, Edan G, Goodkin D, Hartung HP, Lublin FD, et al. Recommended diagnostic criteria for multiple sclerosis: guidelines from the International Panel on the diagnosis of multiple sclerosis. *Ann Neurol* 2001; 50: 121–7.
- McMahon EJ, Bailey SL, Castenada CV, Waldner H, Miller SD. Epitope spreading initiates in the CNS in two mouse models of multiple sclerosis. *Nat Med* 2005; 11: 335–9.
- Miller DH, Barkhof F, Frank JA, Parker GJ, Thompson AJ. Measurement of atrophy in multiple sclerosis: pathological basis, methodological aspects and clinical relevance. *Brain* 2002; 125: 1676–95.
- Paul F, Waiczies S, Wuerfel J, Bellmann-Strobl J, Dorr J, Waiczies H, et al. Oral high-dose atorvastatin treatment in relapsing-remitting multiple sclerosis. *PLoS ONE* 2008; 3: e1928.
- Ransohoff RM, Kivisakk P, Kidd G. Three or more routes for leukocyte migration into the central nervous system. *Nat Rev Immunol* 2003; 3: 569–81.
- Smith SM, Zhang Y, Jenkinson M, Chen J, Matthews PM, Federico A, et al. Accurate, robust, and automated longitudinal and cross-sectional brain change analysis. *Neuroimage* 2002; 17: 479–89.
- Smorodchenko A, Wuerfel J, Pohl EE, Vogt J, Tysiak E, Glumm R, et al. CNS-irrelevant T-cells enter the brain, cause blood-brain barrier disruption but no glial pathology. *Eur J Neurosci* 2007; 26: 1387–98.
- Traboulsee AL, Li DK. The role of MRI in the diagnosis of multiple sclerosis. *Adv Neurol* 2006; 98: 125–46.
- Tran EH, Hoekstra K, van Rooijen N, Dijkstra CD, Owens T. Immune invasion of the central nervous system parenchyma and experimental allergic encephalomyelitis, but not leukocyte extravasation from blood, are prevented in macrophage-depleted mice. *J Immunol* 1998; 161: 3767–75.
- van Horssen J, Bo L, Vos CM, Virtanen I, de Vries HE. Basement membrane proteins in multiple sclerosis-associated inflammatory cuffs: potential role in influx and transport of leukocytes. *J Neuropathol Exp Neurol* 2005; 64: 722–9.
- Vos CM, Geurts JJ, Montagne L, van Haastert ES, Bo L, van der Valk P, et al. Blood-brain barrier alterations in both focal and diffuse abnormalities on postmortem MRI in multiple sclerosis. *Neurobiol Dis* 2005; 20: 953–60.
- Wuerfel J, Bellmann-Strobl J, Brunecker P, Aktas O, McFarland H, Villringer A, et al. Changes in cerebral perfusion precede plaque formation in multiple sclerosis: a longitudinal perfusion MRI study. *Brain* 2004; 127: 111–9.
- Zipp F, Aktas O. The brain as a target of inflammation: common pathways link inflammatory and neurodegenerative diseases. *Trends Neurosci* 2006; 29: 518–27.